Research Square

Preprints are preliminary reports that have not undergone peer review.
They should not be considered conclusive, used to inform clinical practice,
or referenced by the media as validated information.

Clinical, hematological, radiographic, and conventional and elastographic ultrasonographic aspects of the lung and pleura in dogs exposed to tobacco smoke

Giovanna Serpa Maciel Feliciano
giovanna_serpa@hotmail.com
University of Sao Paulo e FZEA - USP
Anna Carolina Mazeto Ercolin
University of Sao Paulo e FZEA - USP
Andriele Pires Suppi
University of Sao Paulo e FZEA - USP
Luiz Paulo Nogueira Aires
University of Sao Paulo e FZEA - USP
Caio Garcia Barbosa Silva
University of Sao Paulo e FZEA - USP
Gabriela Castro Lopes Evangelista
University of Sao Paulo e FZEA - USP
Ana Letícia Baggenstoss
University of Sao Paulo e FZEA - USP
Jennifer Jullie Pichinelli Noronha
University of Sao Paulo e FZEA - USP
Fernando GustavoTonin
University of Sao Paulo e FZEA - USP
Carlos Augusto Fernandes Oliveira
University of Sao Paulo e FZEA - USP
Ricardo Andres Ramirez Uscategui
University of Tolima
Marcus Antônio Rossi Feliciano
University of Sao Paulo e FZEA - USP
Carlos Eduardo Ambrósio
University of Sao Paulo e FZEA - USP

Article

Keywords: Canine, Passive smoking, Radiography, Ultrasonography, Stiffness

Posted Date: November 12th, 2026

DOI: https://doi.org/10.21203/rs.3.rs-11167467/v1

License: This work is licensed under a Creative Commons Attribution 4.0 International License.
Read Full License

Additional Declarations: No competing interests reported.

Abstract

This study evaluated the clinical, hematological, radiographic, B-mode ultrasonographic, and shear-wave elastographic (SWE) characteristics of dogs exposed to tobacco smoke. Seventy dogs were included: 33 unexposed controls (CG) and 37 tobacco smoke-exposed dogs (EG). Clinical and hematological assessments, hair nicotine quantification by liquid chromatography-tandem mass spectrometry, thoracic radiography, pulmonary ultrasonography, and SWE were performed. The EG showed a higher frequency of respiratory clinical signs and higher neutrophil and monocyte counts, total plasma protein and hair nicotine concentrations than the CG ($P < 0.05$). Hair nicotine concentration correlated positively with respiratory clinical manifestations, elastographic findings, and Fagerström Test scores ($P < 0.05$). SWE demonstrated greater pleuropulmonary interface stiffness in the EG, with higher shear-wave velocity (3.89 vs. 3.45 m/s for controls) and predominantly green elastograms compared with predominantly blue elastograms in the CG ($P < 0.05$). Radiographic and B-mode ultrasonographic findings did not differ between groups ($P > 0.05$), with regular pleuropulmonary surfaces, preserved lung sliding, no B-lines, pleural effusion, or masses, and an interface thickness of 0.05 cm. These findings indicate that tobacco smoke exposure in dogs was associated with clinical and laboratory alterations and increased pleuropulmonary interface stiffness, despite the absence of conventional imaging abnormalities that needs attention for public health and type of detection lesions caused by smoking subjects and public around them.

Introduction

The World Health Organization (WHO) has identified the tobacco epidemic as one of the major global public health threats, accounting for more than 7 million deaths annually, approximately 1.6 million of which are attributable to secondhand smoke exposure [1]. In this context, passive exposure to tobacco smoke is particularly relevant for children and companion animals because they spend considerable time with their parents and owners, respectively, and within the household environment [2]. They may also be more exposed to tobacco smoke particles deposited on surfaces, known as thirdhand smoke (THS), because of their characteristic behaviors and close contact with contaminated surfaces [3, 4].

In veterinary medicine, relatively few studies have investigated the effects of environmental tobacco smoke exposure to dogs. Reported effects include chronic cough and increased respiratory secretions [5], an increased risk of pulmonary [6] and nasal neoplasia [7], and, more recently, renal and hepatic alterations in exposed dogs [8, 9].

Tobacco smoking has also been associated with the development of interstitial lung diseases (ILDs), including idiopathic pulmonary fibrosis [10]. When these disorders progress to end-stage pulmonary fibrosis, therapeutic response is often limited, particularly when diagnosis occurs at an advanced stage, regardless of the underlying etiology, emphasizing the importance of early detection [11]. ILDs have also been described in dogs, and cigarette smoke has been proposed as a potential environmental factor associated with pulmonary fibrosis in this species [12].

Thoracic radiography plays an important role in detecting pulmonary disease and potential pulmonary fibrosis in animals; however, radiographic findings are often nonspecific and should therefore be interpreted in conjunction with a complete clinical evaluation and complementary imaging modalities [13]. Thoracic ultrasonography has increasingly contributed to the diagnosis of respiratory diseases in both human and veterinary medicine [14]. Furthermore, elastography has shown potential for the assessment of ILDs and therapeutic monitoring of patients with pulmonary fibrosis in human medicine [15, 16].

Considering that (1) tobacco smoking remains a major public health concern associated with substantial mortality; (2) identifying alterations associated with tobacco smoke exposure in dogs may contribute to the early recognition of pulmonary changes, including those potentially related to ILDs and pulmonary fibrosis; and (3) to our knowledge, no studies have described pulmonary ultrasonographic or elastographic findings of the pleuropulmonary interface in animals exposed to tobacco smoke, we hypothesized that tobacco smoke exposure would be associated with clinical and laboratory alterations, changes in the normal ultrasonographic appearance of the pulmonary and pleural structures, and increased stiffness of the pleuropulmonary interface. Therefore, this study aimed to evaluate the clinical, laboratory, radiographic, B-mode ultrasonographic, and elastographic characteristics of dogs exposed to tobacco smoke, with particular emphasis on the pulmonary structures and pleuropulmonary interface.

Results

Demographic data. The distribution of demographic variables was similar between groups ($P > 0.05$). The overall median age was 7.00 years (IQR: 4.85), with median values of 6.40 years (IQR: 4.28) in the control group (CG) and 7.60 years (IQR: 5.15) in the exposed group (EG). The overall median body weight was 11.66 kg (IQR: 12.50), with values of 11.66 kg (IQR: 17.10) and 11.50 kg (IQR: 11.30) in the CG and EG, respectively. The median body condition score (BCS) was 5.00 (IQR: 2.00) overall, 5.00 (IQR: 1.00) in the CG, and 6.00 (IQR: 2.00) in the EG. Sex distribution was also similar between groups, with the CG comprising 52% females and 48% males and the EG comprising 54% females and 46% males.

Mixed-breed dogs were the most frequently represented (23/70; 32.8%), followed by Beagles (11/70; 15.7%), Border Collies (5/70; 7.1%), Brazilian Terriers (5/70; 7.1%), Dachshunds (4/70; 5.7%), Shih Tzus (4/70; 5.7%), and other breeds (18/70; 25.7%).

Clinical and hematological data. Baseline heart rate was significantly higher in the EG, with a median of 108 beats/min (IQR: 23), compared with 96 beats/min (IQR: 34) in the CG ($P = 0.041$). Respiratory rate did not differ significantly between groups ($P = 0.064$), with median values of 32 breaths/min (IQR: 80) in the CG and 48 breaths/min (IQR: 72) in the EG. Respiratory clinical signs were significantly more frequent in dogs exposed to tobacco smoke ($P < 0.001$). All other physical examination parameters, including cardiac and pulmonary auscultation, thoracic percussion, body temperature, capillary refill time, mucous membrane color, superficial lymph node assessment, and skin turgor, were within clinically acceptable limits in both groups.

Regarding hematological findings, tobacco smoke-exposed dogs had significantly higher total plasma protein concentrations ($P < 0.001$) and circulating neutrophil ($P = 0.047$) and monocyte ($P = 0.014$) counts than dogs in the CG (Table 1). No significant between-group differences were detected for the remaining hematological variables ($P > 0.05$).

Table 1
Median and interquartile range (IQR) of hematological parameters in dogs from the control (CG) and tobacco smoke-exposed (EG) groups.

Parameters	Group	Median	IQR	Asymmetry	P-value
Red blood cells (×10⁶/μL)	CG	7,340	0,715	0,36	0,769
	EG	7,410	0,985	-1,49	
Hemoglobin (g/dL)	CG	17,600	3,200	0,22	0,378
	EG	17,600	3,200	-0,99	
Hematocrit (%)	CG	51,000	8,200	-0.17	0,809
	EG	51,90	9,40	-1,33	
Total plasma protein (g/dL)	CG	7,000	1,000	-3,13	< 0,001*
	EG	8,000	1,500	0,55	
Platelets (/μL)	CG	364000	129000	0,73	0,404
	EG	349000	255500	0,14	
Total leukocytes (/μL)	CG	8400	2250	0,10	0,135
	EG	9000	4150	0,81	
Neutrophils (/μL)	CG	5623	2360	0,19	0,047*
	EG	6570	2730	1,10	
Eosinophils (/μL)	CG	352,0	530,5	1,27	0,601
	EG	410,0	424,0	3,17	
Basophils (/μL)	CG	0,000000	0,000000	0,000000	0,856
	EG	0,00	0,00	6,08	
Lymphocytes (/μL)	CG	1675	1326	0,39	0,427
	EG	1566	949	3,13	
Monocytes (/μL)	CG	260,0	342,5	1,01	0,014*
	EG	364,0	469,5	1,39	

Abbreviations: CG, control group; EG, tobacco smoke-exposed group.

P-values refer to comparisons between the CG and EG using the Mann–Whitney test. *Statistical significance was set at P < 0.05.

Radiographic and ultrasonographic findings. The occurrence of a radiographic pulmonary pattern and visualization of pleural fissure lines did not differ significantly between groups (P = 0.198 and P = 0.667,

respectively). In the CG, 79% of dogs had no detectable abnormal pulmonary pattern, whereas 21% exhibited a bronchial pattern. In the EG, 65% had no detectable abnormal pulmonary pattern, whereas a bronchial pattern was identified in 35%. All visualized pleural fissure lines were thin. Pleural fissure lines were identified in 30% and 35% of dogs in the CG and EG, respectively, and were not identified in 70% and 65%, respectively.

On B-mode ultrasonography, the pleuropulmonary interface was regular in all dogs, with no pleural effusion, subpleural masses, or B-lines identified. Lung sliding and A-lines were present, and the "gator sign" was preserved across all evaluated thoracic regions in 100% of dogs in both groups ($P > 0.05$) (Fig. 1). Pleuropulmonary interface thickness measured on B-mode ultrasonography did not differ significantly between the EG and CG in any of the evaluated regions ($P > 0.05$), with measurements remaining approximately 0.05 cm across regions (Table 2).

Table 2
Median and interquartile range (IQR) of pleuropulmonary interface thickness in dogs from the control (CG) and tobacco smoke-exposed (EG) groups across the different regions evaluated by B-mode ultrasonography.

Variable	Group	Median (cm)	IQR	Asymmetry	P-value
Left CD	CG	0,05	0,01	1,00	0,672
	EG	0,05	0,01	1,50	
Left PH	CG	0,05	0,01	1,19	0,613
	EG	0,05	0,01	1,80	
Left MD	CG	0,05	0,01	1,26	0,698
	EG	0,05	0,00	1,22	
Left CR	CG	0,05	0,01	1,07	0,634
	EG	0,05	0,01	0,62	
Right CD	CG	0,05	0,01	1,77	0,707
	EG	0,05	0,01	1,36	
Right PH	CG	0,05	0,01	1,33	0,373
	EG	0,05	0,00	0,00	
Right MD	CG	0,05	0,00	2,02	0,746
	EG	0,05	0,01	0,81	
Right CR	CG	0,05	0,00	2,02	0,930
	EG	0,05	0,00	1,54	

Abbreviations: CG, control group; EG, tobacco smoke-exposed group; CD, caudodorsal region; PH, perihilar region; MD, middle region; CR, cranial region; IQR, interquartile range.

P-values refer to comparisons between the CG and EG using the Mann–Whitney test. *Statistical significance was set at $P < 0.05$.

On qualitative elastographic assessment, the elastographic pattern of the pleuropulmonary interface was homogeneous in all evaluated regions in 100% of dogs from both groups ($P > 0.05$). However, the pleuropulmonary interface exhibited significantly greater apparent stiffness in tobacco smoke-exposed dogs across all evaluated regions ($P < 0.05$). The elastograms of dogs in the EG were predominantly green, whereas those of dogs in the CG predominantly exhibited blue tones, consistent with comparatively lower apparent stiffness.

For quantitative SWE assessment, ROIs were positioned only within homogeneous areas of the elastogram with adequate measurement reliability. Shear-wave velocity (SWV; m/s) measurements

obtained at the pleuropulmonary interface were significantly higher in tobacco smoke-exposed dogs than in control dogs across all evaluated thoracic regions (P < 0.05) (Table 3). When measurements were compared among the different thoracic regions, neither pleuropulmonary interface thickness (P = 0.7586) nor SWV (P = 0.1527) differed significantly among regions. Given the absence of significant regional differences, global median values were subsequently calculated for an integrated between-group comparison. Global pleuropulmonary interface thickness did not differ between the EG and CG (P = 0.962), with an overall median of 0.05 cm (IQR: 0.01). In contrast, global SWV of the pleuropulmonary interface was significantly higher in the EG than in the CG (P < 0.01), with median values of 3.89 m/s (IQR: 0.79) and 3.45 m/s (IQR: 0.89), respectively (Figs. 2 and 3).

Table 3
Median and interquartile range (IQR) of the shear-wave velocity (SWV) of the pleuropulmonary interface of dogs from the control (CG) and tobacco smoke-exposed (EG) groups across the different regions evaluated by elastography

Variable	Group	Median (m/s)	IQR	Asymmetry	P-value
Left CD	CG	3,34	0.84	0,27	0,006*
	EG	3,76	1,13	0,31	
Left PH	CG	3,16	0,98	0,46	< 0,001*
	EG	3,85	0,93	0,50	
Left MD	CG	3,56	0,98	-0,07	< 0,001*
	EG	4,12	1,02	0,29	
Left CR	CG	3,51	0,95	0,00	< 0,001*
	EG	4,00	0,86	-0,03	
Right CD	CG	3,44	1,09	-0,38	0,001*
	EG	3,94	1,10	0,53	
Right PH	CG	3,09	0,90	0,79	< 0,001*
	EG	3,86	0,89	0,67	
Right MD	CG	3,31	1,04	-0,13	< 0,001*
	EG	4,03	0,78	0,57	
Right CR	CG	3,45	0,88	-0,21	0,001*
	EG	3,90	1,00	0,06	

Abbreviations: CG, control group; EG, tobacco smoke-exposed group; CD, caudodorsal region; PH, perihilar region; MD, middle region; CR, cranial region; IQR, interquartile range.

P-values refer to comparisons between the CG and EG using the Kruskal-Wallis test. *Statistical significance was set at P < 0.05.

Hair nicotine concentration and correlation analyses. Quantitative measurement of nicotine in hair confirmed tobacco smoke exposure in the study group. Hair nicotine concentration was significantly higher in the EG (median: 0.11 ng/mL; IQR: 0.58) than in the CG ($P < 0.001$), in which nicotine was not detected (median: 0.00 ng/mL; IQR: 0.00) (Fig. 4).

Correlation analyses were performed between hair nicotine concentration and variables that differed significantly between the CG and EG. Hair nicotine concentration showed significant positive, moderate correlations (Spearman's $r = 0.3–0.7$; $P < 0.05$) with respiratory clinical signs, qualitative elastographic findings, and SWV measurements of the pleuropulmonary interface (Table 4).

Table 4
Spearman correlations between hair nicotine concentration and respiratory clinical signs (RCS), elastogram findings, and shear-wave velocity (SWV) of the pleuropulmonary interface in dogs from the tobacco smoke-exposed group.

Variable	Statistics	Nicotine concentration
RCS	Spearman's r	0,471
	P-value	< 0,001*
Left CD elastogram	Spearman's r	0,286
	P-value	0,027*
Left PH elastogram	Spearman's r	0,356
	P-value	0,004*
Left MD elastogram	Spearman's r	0,399
	P-value	0,002*
Left CR elastogram	Spearman's r	0,386
	P-value	0,002*
Right CD elastogram	Spearman's r	0,321
	P-value	0,011*
Right PH elastogram	Spearman's r	0,424
	P-value	0,001*
Right MD elastogram	Spearman's r	0,318
	P-value	0,013*
Right CR elastogram	Spearman's r	0,317
	P-value	0,013*
Pleuropulmonary interface SWV	Spearman's r	0,409
	P-value	0,001*

Abbreviations: RCS, respiratory clinical signs; SWV, shear-wave velocity; CD, caudodorsal region; PH, perihilar region; MD, middle region; CR, cranial region. *Statistically significant at the 5% significance level according to Spearman's rank correlation test.

The exposure scale score (Spearman's $r = 0.657$; $P < 0.001$) and Fagerström Test score (Spearman's $r = 0.786$; $P < 0.001$) were significantly and positively correlated with hair nicotine concentration.

Discussion

Exposure to tobacco smoke was potentially detrimental to canine health, as demonstrated by clinical and laboratory alterations and changes in the mechanical properties of the pleuropulmonary interface detected by elastography. These findings suggest a potential role for elastography in the early detection of tissue alterations, including those potentially associated with pulmonary fibrotic processes. In addition to demonstrating potential adverse effects of tobacco smoke exposure on canine health, these results may increase awareness of the risks of passive exposure and encourage measures to reduce tobacco smoke exposure in companion animals.

The higher heart rate observed in the exposed group is consistent with findings in nonsmoking humans passively exposed to tobacco smoke compared with unexposed individuals and may be related to increased sympathetic stimulation [17, 18]. Nicotine may contribute to this cardiovascular response through activation of the sympathetic nervous system, resulting, among other effects, in an increased heart rate [19]. In nonsmoking humans passively exposed to tobacco smoke compared with unexposed individuals and may be related to increased sympathetic stimulation [17, 18]. Nicotine may contribute to this cardiovascular response through activation of the sympathetic nervous system, resulting, among other effects, in an increased heart rate [19].

Respiratory rate did not differ between groups, consistent with other authors, who also found no difference in respiratory rate between dogs exposed and unexposed to environmental tobacco smoke [5]. However, these authors identified changes in other parameters assessed by whole-body barometric plethysmography, suggesting greater airway limitation in exposed dogs. Similarly, in human patients, respiratory rate did not differ between active smokers and nonsmokers [20] or between individuals with and without passive tobacco smoke exposure during exercise [21]. These findings indicate that tobacco smoke-related respiratory dysfunction may occur even in the absence of changes in respiratory rate.

No adventitious lung sounds were detected in either group. Similarly, another study, using recorded lung sounds subsequently analyzed by spectrogram, reported no wheezes or crackles in 62.7% of active smokers [22]. Thus, adventitious sounds may be absent even in actively exposed individuals, suggesting that their absence may also occur with passive exposure, as observed in the present study. Moreover, normal pulmonary auscultation does not exclude underlying pulmonary abnormalities [23].

Environmental tobacco smoke may contribute to and exacerbate chronic cough in dogs with respiratory disease, with chemical and physical injury from smoke exposure potentially increasing respiratory secretion production [5]. In passive smokers, both greater intensity and longer duration of tobacco smoke exposure have also been associated with an increased likelihood of respiratory symptoms [24]. These observations support a possible association between tobacco smoke exposure and the higher frequency of respiratory clinical signs observed in exposed dogs in the present study.

The higher total plasma protein concentrations and neutrophil and monocyte count in tobacco smoke-exposed dogs may reflect changes in individual plasma protein fractions, such as albumin, globulins, and fibrinogen, as well as an inflammatory response. Higher albumin concentrations were reported in smokers [25], consistent with the higher total plasma protein concentrations observed in the present

study. During inflammation, concentrations of positive acute-phase proteins, including fibrinogen, increase [26, 27], potentially contributing to increased total plasma protein concentrations. Although fibrinogen was not specifically measured in the present study, this hypothesis is supported by studies in humans in which higher fibrinogen concentrations were associated with passive tobacco smoke exposure [28, 29].

The higher neutrophil and monocyte count in the exposed group may be related to increased myeloid cell production in the bone marrow and consequently greater availability of these cells in the circulation in response to cigarette smoke exposure [30]. Higher circulating neutrophil counts have similarly been reported in active smokers compared with nonsmokers [31, 32]. Increased monocyte counts have also been observed in active smokers [33, 34], with positive associations reported between monocyte counts and cumulative cigarette exposure, expressed as pack-years, as well as smoking duration (years) [35].

Thoracic radiography revealed no significant differences in pulmonary patterns between groups. Although this finding may suggest a lack of association between tobacco smoke exposure and detectable radiographic pulmonary abnormalities, the bronchial pattern observed in both groups is nonspecific and may occur with several conditions, including allergic disease, aging, and exposure to inhaled irritants [36]. The present study also provided a better characterization of tobacco smoke exposure including the exposure duration, number of smokers, and characteristics of the exposure environment.

The frequency of thin pleural fissure lines on thoracic radiographs did not differ between groups. Thin pleural fissure lines may be visible under normal conditions when the X-ray beam is tangential to the interlobar pleura but may also occur with mild pleural thickening [37], small volumes of pleural fluid [38], or mild pleural fibrosis [39, 40]. Therefore, because pleural fissure lines may occur both physiologically and in association with pleural disease, this nonspecific finding may explain the absence of a difference between groups.

B-mode ultrasonographic findings were predominantly consistent with a normal pleuropulmonary appearance. Regarding pleural surface regularity, another study reported an association between active smoking and pleural line irregularity in humans [41]. Other authors described pleural irregularity in 85% of patients with idiopathic pulmonary fibrosis (IPF), in a population in which 52.5% were smokers [42]. In veterinary medicine, however, there was no difference in the occurrence of pleural irregularities between dogs with canine idiopathic pulmonary fibrosis and healthy controls [43]. Thus, although pleural irregularity has been associated with smoking in humans, such an association was not evident in the tobacco smoke-exposed dogs evaluated in the present study.

Although pleural thickening may occur in fibrotic processes [44] and smoking may contribute to fibrotic pulmonary abnormalities [45], increased pleuropulmonary interface thickness was not observed in the present study. Similarly, no association was found between smoking and thickened or irregular pleural lines or small subpleural consolidations in humans [46]. Using computed tomography, other authors also found no significant difference in pleural thickening between smokers and nonsmokers [47]. Collectively,

these findings suggest that tobacco smoke exposure is not necessarily accompanied by detectable pleural thickening, consistent with the findings in the exposed dogs in this study.

Lung sliding remained present in both control and exposed dogs. In active smokers, pleural adhesions may develop secondary to excessive exudation associated with chronic inflammation [48], and absent lung sliding may be associated with such adhesions [49]. However, lung sliding may remain preserved even in fibrotic pulmonary disease. Normal lung sliding was reported in 82.5% of patients with IPF, in a population comprising 52.5% smokers [42]. Similarly, lung sliding remained present in dogs with canine idiopathic pulmonary fibrosis, which the authors suggested could reflect less severe remodeling of pulmonary architecture [43]. Therefore, although pleural adhesions may be associated with smoking, tobacco smoke exposure does not necessarily result in reduced or absent lung sliding, and this sign may remain preserved even in pulmonary fibrotic disease in humans and dogs.

Although smoking may be associated with pleural inflammation, pleural effusion was not detected in exposed dogs. In active smokers, an increased proportion of neutrophils has been reported in pleural fluid obtained by pleural lavage. Conversely, other authors identified smoking as one of the factors associated with smaller volumes of pleural fluid on magnetic resonance imaging [50], while no significant difference in the occurrence of pleural effusion on computed tomography was reported between smokers and nonsmokers [47]. These findings suggest that although smoking may induce inflammatory pleural changes, these alterations are not necessarily accompanied by the development or accumulation of detectable pleural fluid.

The gator sign remained preserved in both groups, with no detectable ultrasonographic abnormalities. Regarding reverberation artifacts, A-lines were present and B-lines were absent in both groups. A-lines are predominantly observed in normally aerated lungs [14], whereas B-lines may occur as either physiological or pathological findings depending on their number and distribution [51]. Another study found no significant difference in the presence of B-lines between smokers and nonsmokers (31% vs. 11%, respectively), with a single B-line observed in most participants (84%) [52]. However, B-lines were identified in all patients with IPF in another study, regardless of smoking status [42]. Therefore, preservation of the gator sign, presence of A-lines, and absence of B-lines were consistent with a normal lung ultrasound appearance in both groups, suggesting that B-lines may be more strongly associated with underlying pulmonary disease than with tobacco smoke exposure itself.

No subpleural masses were identified in either group. There was reported an association between tobacco smoke exposure and lung cancer in brachycephalic and mesocephalic dogs [6]. Conversely, other authors found no significant association between secondhand tobacco smoke exposure and primary lung cancer in dogs in a study including 2.6 times more cases and four times more controls [53]. In humans, cigarette smoking is strongly associated with lung cancer risk [54], while secondhand smoke exposure increases this risk by more than 20% [55]. Thus, unlike the well-established relationship between active or passive smoking and lung cancer in humans, current evidence regarding passive

tobacco smoke exposure and canine primary lung cancer, in both literature and in the present study, remains inconsistent.

Qualitative elastography demonstrated greater apparent stiffness of the pleuropulmonary interface in tobacco smoke-exposed dogs, characterized by predominantly green tones on the elastograms, whereas control dogs showed predominantly blue elastograms across all evaluated regions. Patients with interstitial lung disease, including IPF and other idiopathic interstitial pneumonias presented greater apparent stiffness of the superficial lung region compared with controls, demonstrated by a predominance of colors indicative of increased stiffness [56]. The authors suggested that this finding could be related to pulmonary fibrosis. These observations support the ability of qualitative elastography to identify changes in the mechanical properties of superficial pulmonary tissues and suggest that underlying tissue alterations may similarly contribute to the greater apparent stiffness observed in tobacco smoke-exposed dogs.

Quantitative elastography further demonstrated higher shear-wave velocity (SWV; m/s) at the pleuropulmonary interface in tobacco smoke-exposed dogs across all evaluated anatomical regions, indicating greater stiffness compared with controls. One possible explanation is that chronic cigarette smoke exposure may promote pulmonary fibrotic processes [45], which are associated with altered tissue mechanical properties [57]. Cigarette smoke induces oxidative stress and promotes the release of pro-inflammatory and profibrotic mediators, including TGF-β1, stimulating fibroblast proliferation and differentiation into myofibroblasts. These processes promote extracellular matrix (ECM) deposition, particularly collagen, within the pulmonary parenchyma and may ultimately contribute to pulmonary fibrosis [45]. Increased stiffness of fibrotic lung tissue may result from ECM accumulation, alterations in collagen fiber organization, and increased collagen cross-linking [57]. Collectively, these findings support the hypothesis that chronic passive tobacco smoke exposure may induce tissue remodeling that contributes to the increased pleuropulmonary interface stiffness detected in exposed dogs.

Although biopsy and histopathological evaluation of the pulmonary regions corresponding to the elastographic assessment were not performed, the presence of inflammatory findings, evidenced by increased neutrophil and monocyte counts and total plasma protein concentrations, together with the increased stiffness of the pleuropulmonary interface in tobacco smoke-exposed dogs, suggests the possibility of interstitial lung disease (ILD). This interpretation is supported by the fact that ILDs are characterized by inflammatory and fibrotic processes and that cigarette smoke has been proposed as a potential environmental factor associated with pulmonary fibrosis in dogs [12].

Hair nicotine concentrations were higher in exposed dogs, whereas nicotine was not detected in controls. Similarly, differences in hair nicotine concentrations were associated with tobacco smoke exposure category, with the highest concentrations in regularly exposed dogs [58]. Likewise, other authors observed increasing hair nicotine concentrations with greater tobacco smoke exposure [59]. These findings support the association between nicotine concentration and tobacco smoke exposure and its use as an exposure biomarker. In the present study, hair nicotine quantification complemented

owner-reported questionnaire data by providing an objective quantitative measure of tobacco smoke exposure.

The moderate positive correlation between hair nicotine concentration and respiratory clinical manifestations is consistent with another study that reported an association between hair nicotine concentration and a higher frequency of respiratory symptoms in women passively exposed to tobacco smoke [60]. Higher urinary cotinine concentrations were also described in children presenting with cough, rhinorrhea, and sneezing [61]. These findings indicate that higher concentrations of tobacco smoke exposure biomarkers may be associated with the presence or greater frequency of respiratory symptoms and support the relationship observed in the present study

Both qualitative and quantitative elastographic findings showed moderate positive correlations with hair nicotine concentration, suggesting that greater tobacco smoke exposure was associated with increased pleuropulmonary interface stiffness in dogs. To our knowledge, this association has not previously been investigated in either active smokers or passively exposed individuals. These findings therefore provide novel information regarding the potential effects of tobacco smoke exposure on the mechanical properties of the pleuropulmonary interface.

The positive correlation between hair nicotine in dogs and the Fagerström Test of their owners indicates that greater nicotine dependence among smokers was associated with greater tobacco smoke exposure in their dogs. Although most smokers were classified as having low (62.5%) nicotine dependence, exposure of the dogs was objectively demonstrated. This corroborates studies with dogs [62] and children [63], indicating that passive exposure may occur even when smokers have a low degree of nicotine dependence and represents real health risk. This is further supported by the clinical and laboratory alterations and increased pleuropulmonary interface stiffness detected in exposed dogs of the present study. The strong correlation between the exposure scale and hair nicotine indicates that indoor smoking and higher number of smokers increase the dogs' exposure. This finding was like a previous study describing that nicotine concentrations in women and children increased (1.8 and 2.6-fold higher) with the number of smokers in the household [64]. Together, these findings support the exposure scale used in the present study and emphasize the influence of household smoking characteristics on passive tobacco smoke exposure in dogs.

Methods

Ethical aspects. This project was approved by the Ethics Committee on Animal Use of the Faculty of Animal Science and Food Engineering, University of São Paulo, Pirassununga, São Paulo, Brazil (CEUA/FZEA/USP, No. 5248010623) and all experiments were performed in accordance with relevant guidelines and regulations. Additionally, this project was approved by the Research Ethics Committee for studies involving human participants (CEP/FZEA/USP, No. 6.435.293) and all experiments were performed in accordance with relevant guidelines and regulations. A prospective study was conducted using client-owned dogs from Pirassununga, São Paulo, Brazil, and animals presented to the Veterinary

Hospital (HOVET - FZEA/USP). Before enrollment, owners received detailed information regarding the study objectives and procedures and provided written informed consent for their dogs' participation. Owners who smoked participated in an exposure assessment, providing written consent for their own participation. The animals were not sedated, anesthetized, or euthanized and returned to their homes after the experimental collections.

Study design andanimals. Seventy adult dogs aged ≥ 2 years were prospectively enrolled and allocated to either the control group (CG; n = 33) or the tobacco smoke-exposed group (EG; n = 37). CG comprised clinically healthy dogs with no known exposure to commercial cigarette smoke, no abnormalities detected on clinical and physical examinations, and no history of acute or chronic cardiopulmonary disease or malignant neoplasia. The EG comprised dogs with a history of exposure to commercial cigarette smoke for at least one year. Dogs in this group could present with or without clinical signs suggestive of chronic respiratory disease, including coughing, dyspnea, increased abdominal respiratory effort, and exercise intolerance. Dogs with a history of cardiac diseases, recent acute pulmonary disease, or malignant neoplasia were excluded.

Clinical assessment. Before diagnostic imaging, all dogs underwent anamnesis, physical examination, complete blood count (CBC), and hair collection for nicotine quantification. In addition, owners of dogs in the EG completed questionnaires designed to characterize nicotine dependence and the degree of environmental tobacco smoke exposure.

During anamnesis, information was obtained regarding signalment, home environment, management, medical history, and general health status. Attention was given to respiratory clinical signs, including coughing, sneezing, respiratory distress, exercise intolerance or easy fatigability, and nasal discharge. A clinical respiratory score was established according to the number of reported signs and categorized as follows: absent (0 signs), mild (1 to 2 signs), moderate (3 to 4 signs), or severe (5 to 6 signs).

Smoking owners were assessed for nicotine dependence using the Fagerström Test for Nicotine Dependence (FTND) [65]. The FTND consists of six questions scored from 0–1 or 0–3, yielding a total score ranging from 0 to 10 [66]. Nicotine dependence was categorized according to the total score as very low (0–2), low (3–4), moderate (5), high (6–7), or very high (8–10) [67].

An additional questionnaire was developed to characterize the degree of tobacco smoke exposure of each dog according to the number of smokers in the household and the environment in which exposure occurred. Exposure was scored as follows: 0, no exposure to tobacco smoke; 1, one smoker, with the dog exposed predominantly or exclusively outdoors; 2, more than one smoker, with the dog exposed predominantly or exclusively outdoors; (3) one smoker, with the dog exposed both indoors and outdoors; (4) more than one smoker, with the dog exposed both indoors and outdoors; (5) one smoker, with the dog exposed exclusively indoors; (6) more than one smoker, with the dog exposed exclusively indoors.

Physical examination included assessment of body temperature, cardiac and pulmonary auscultation, thoracic percussion, thoracic wall abnormalities, capillary refill time (CRT), mucous membrane color,

superficial lymph nodes, and skin turgor. Pulmonary auscultation was specifically assessed for abnormal respiratory sounds, including stridor and crackles, as well as areas of reduced or absent breath sounds. Thoracic percussion was evaluated for abnormal resonance, including areas of dullness. The thoracic wall was inspected and palpated for abnormalities such as swelling or nodules, and dogs were examined for clinically detectable neoplastic lesions at other sites, including mammary masses. A CBC was performed to assess general health status and identify hematological abnormalities potentially associated with respiratory disease, including changes suggestive of inflammatory, infectious, or hemorrhagic processes.

For quantitative nicotine analysis, approximately 120 mg of hair was collected after clipping the thoracic region. Samples were vacuum-sealed and stored at − 20°C until analysis. Hair nicotine concentration (ng/mg) was determined by ultra-performance liquid chromatography coupled with tandem mass spectrometry (UPLC-MS/MS) at the Food Microbiology and Mycotoxicology Laboratory (LMMA) of FZEA/USP.

Following clinical and laboratory assessment, dogs from both groups underwent diagnostic imaging examinations in the following sequence: 1) thoracic radiography, 2) B-mode thoracic ultrasonography, and 3) shear-wave elastography (SWE). Data obtained from the anamnesis, questionnaire responses, physical examination, and laboratory findings were recorded for each dog on a standardized study form. Each dog was subsequently assigned a random identification number used for radiographic and ultrasonographic image assessment. Ultrasonographic examinations were also recorded as video clips for subsequent review. Image datasets were identified only by the assigned numerical code during interpretation, thereby allowing blinded image analysis with respect to group allocation and clinical information.

Radiographic examination. Thoracic radiography preceded ultrasonographic and elastographic evaluations. In clinically unstable patients, radiographs were obtained only after appropriate clinical stabilization to minimize risks associated with positioning and restraint. Thoracic radiographs were acquired using an Altus ST 543 HF X-ray unit and a DIGIX WM digital radiography system. Three standard projections were obtained whenever clinically feasible: left lateral, right lateral, and ventrodorsal. Images were acquired at peak inspiration, with exposure parameters (kVp and mAs) adjusted according to patient size.

Images were obtained using a cassette for digital reading suitable for the patient's thoracic size. Digital radiographs were stored in Digital Imaging and Communications in Medicine (DICOM) format and subsequently reviewed using dedicated DICOM viewing software (Digital Imaging and Communications in Medicine, Rosslyn, VA, USA) and archived for subsequent analysis. Radiographic evaluation of pulmonary parenchyma included assessment for bronchial, interstitial (unstructured or structured), alveolar, and vascular pulmonary patterns. When features of more than one pulmonary pattern were simultaneously present, the findings were classified as a mixed pulmonary pattern [68].

A bronchial pattern was characterized by increased visibility and thickening of the bronchial walls, bronchial dilation, and an increased number and conspicuity of end-on (“donuts”) and longitudinal (“tram tracks”) bronchial profiles. An unstructured interstitial pattern was defined as a mild-to-moderate diffuse or regional increase in pulmonary opacity without clearly defined margins, whereas a structured interstitial pattern was characterized by identifiable nodular or miliary pulmonary opacities. An alveolar pattern was characterized by increased soft-tissue pulmonary opacity associated with lobar signs, air bronchograms, and border effacement of adjacent structures. A vascular pattern was defined by an abnormal increase or decrease in the diameter of the pulmonary vessels.

The pleural space was additionally evaluated for the presence or absence of visible pleural fissure lines.

Ultrasound assessment. For ultrasonographic examination, the hair was extensively clipped over the right and left thoracic walls to optimize acoustic coupling and allow systematic assessment of both hemithoraces. In clinically unstable patients, for which minimal restraint and rapid examination were prioritized, focal clipping was performed according to the suspected lesion location based on clinical, physical examination, and radiographic findings and was extended as necessary during the examination.

Following clipping, patients were manually restrained with the head oriented toward the ultrasound monitor and the body positioned parallel to the ultrasound system. Examinations were performed with the animals in right or left lateral recumbency, sternal recumbency, or a standing position, depending on the acoustic window required and the patient’s clinical and respiratory condition. Patient positioning and restraint were adapted to minimize stress and avoid respiratory distress.

Ultrasound coupling gel was applied to the skin before image acquisition. In dyspneic or unstable patients requiring minimal manipulation and continuous monitoring, ultrasonography was performed while supportive oxygen therapy was maintained when indicated. In patients requiring general anesthesia as part of their clinical management, ultrasonographic assessment could also be performed following orotracheal intubation and anesthetic stabilization, according to the decision of the attending emergency and anesthesia teams.

All examinations were performed using a MyLab X90 ultrasound system (Esaote, Italy) equipped with an LX 3–15 multifrequency linear-array transducer (3–15 MHz). To ensure systematic evaluation of both hemithoraces, the scanning protocol incorporated the acoustic windows described in the Vet BLUE protocol [69]. Four regions were assessed in each hemithorax: caudodorsal (CD), perihilar (PH), middle (MD), and cranial (CR), resulting in a total of eight thoracic regions. The CD region was evaluated at the eighth or ninth intercostal space in the dorsal third of the thorax; the PH region between the sixth and seventh intercostal spaces in the middle third; the MD region between the fourth and fifth intercostal spaces in the ventral third; and the CR region at the second or third intercostal space in the ventral third of the thorax [70]. At each acoustic window, the transducer was positioned within the intercostal spaces in both transverse and longitudinal orientations relative to the accessible pleuropulmonary surface and peripheral lung fields.

B-mode ultrasonography. B-mode ultrasonography was used to evaluate the lung surface (pleuropulmonary interface) and peripheral lung fields [71]. The pleuropulmonary interface was assessed for surface regularity (regular or irregular), thickness (cm), presence or absence of pleural effusion, characteristics of pleural fluid when present (anechoic or echogenic, with or without suspended echogenic material/debris), presence or absence of lung sliding (sliding sign), and presence or absence of subpleural masses. The peripheral lung fields were additionally assessed for the presence of the "gator sign" and A-lines. The "gator sign" was identified with the transducer oriented transversely to the ribs and was characterized by acoustic shadowing produced by two adjacent ribs (“gator eyes”) separated by the intercostal space (“gator snout”), within which the pleuropulmonary interface was visualized. A-lines were defined as horizontal, hyperechoic reverberation artifacts located deep and parallel to the pleuropulmonary interface and recurring at regular intervals.

Shear-wave elastography (SWE). Following B-mode assessment, SWE was performed using the same ultrasound system and transducer by activating the dedicated elastography software (used for both qualitative and quantitative investigations). Elastographic evaluation was conducted at the same CD, PH, MD, and CR regions of the right and left hemithoraces assessed during B-mode ultrasonography.

For each region, the system-generated reliability map was first evaluated to ensure adequate shear-wave propagation and measurement quality. The reliability map was displayed using green, yellow, and orange coding, corresponding to high, intermediate, and low measurement reliability, respectively. Only areas displaying green coding were considered suitable for qualitative assessment and quantitative measurements (Fig. 5).

A color-coded elastogram was subsequently obtained using a stiffness scale set to 10. Tissue stiffness was displayed using a color spectrum ranging from dark blue to red, with dark blue, light blue, green, yellow, and red representing progressively increasing stiffness. The color pattern of the pleuropulmonary interface was qualitatively assessed and classified as homogeneous or heterogeneous according to the distribution of colors within the elastogram.

For quantitative SWE assessment, five circular regions of interest (ROIs), each 0.2 cm in diameter, were positioned at the pleuropulmonary interface within areas demonstrating adequate reliability. Shear-wave velocity (SWV), expressed in m/s, was automatically calculated by the software for each ROI. The median SWV of five measurements was subsequently calculated and used as the representative value for each thoracic region (Fig. 5) [72].

Quantitative analysis of nicotine in hair by ultra-performance liquid chromatography coupled with tandem mass spectrometry (UPLC-MS/MS). Sample preparation was performed according to literature [73], with minor modifications. In a Petri dish, 35.0 mg of the sample was weighed and subsequently transferred to a 4-mL capped glass vial, to which 2 mL of HPLC-grade methanol was added. The vial was hermetically sealed and subjected to ultrasonic extraction for 120 minutes at room temperature. The resulting extract was filtered through a 0.22-μm PTFE membrane. Subsequently, 20 μL of a 200 ng/mL nicotine-d4 solution in methanol was added to 980 μL of the filtrate, resulting in a final concentration of

4.0 ng/mL of the isotopically labeled internal standard. Following the addition of the internal standard, the sample was directly analyzed.

Nicotine determination was performed using an LC-MS/MS system consisting of an Acquity I-Class™ ultra-performance liquid chromatograph (UPLC; Waters Corp., Milford, MA, USA) coupled to a Xevo TQS™ triple-quadrupole mass spectrometer (MS/MS) equipped with an electrospray ionization (ESI) (Waters Corp., Milford, MA, USA). Chromatographic separation was achieved using a SeQuant ZIC®-HILIC analytical column (150 x 2.1 mm, 3.5 µm; Merck) coupled to a SeQuant ZIC®-HILIC guard column (20 x 2.1 mm; Merck). The system was operated at a flow rate of 0.3 mL/min and a column temperature of 40°C. The mobile phase consisted of water (phase A) and acetonitrile (phase B), both containing 5,0 mmol/Lammonium acetate and 0.1% acetic acid.

Gradient elution was performed as follows: 80% phase B was maintained for the first 1 min, followed by a linear decrease to 50% phase B at 7 min. The proportion of phase B was then returned to 80% at 8 min and maintained until 20 min to allow column re-equilibration, resulting in a total run time of 20 min. The injection volume was 5 µL for both samples and calibration standards.

Detection and quantification were performed using Multiple Reaction Monitoring (MRM) in positive mode $(M + H)^+$. The mass spectrometer was operated under the following conditions: capillary voltage, 3.0 kV; source temperature, 150°C; desolvation temperature, 400°C; desolvation gas flow rate, 800 L/h; and cone gas flow rate, 150L/h. Cone voltages and collision energies were manually optimized for each MRM transition (precursor ion → fragment ion).

Quantification was performed using a matrix-matched calibration curve and isotope dilution methodology, with nicotine-d4 as the isotopically labeled internal standard. The instrumental limits of detection (LOD, S/N = 3) and quantification (LOQ, S/N = 10) were estimated at 0.15 and 0.50 ng/mL, respectively. Based on the sample preparation procedure and instrumental limits, the method limits of detection (MLOD) and quantification (MLOQ) were estimated at 0.009 ng/mg and 0.029 ng/mg of hair, respectively. Seven calibration levels were prepared for nicotine at concentrations of 0.50, 0.75, 1.0, 2.0, 4.0, 10, and 20 ng/mL, each containing 4.0 ng/mL of nicotine-d4. The calibration curve was fitted using weighted linear regression (1/x) and yielded a coefficient of determination (R^2) of 0.998. The absence of systematic bias and the agreement between predicted and nominal concentrations were also evaluated. Data processing was performed using MassLynx software, version 4.1.

Statistical analysis. Statistical analyses were performed using R software (R Foundation for Statistical Computing). The normality of quantitative data was initially assessed using the Shapiro–Wilk test. As most of the quantitative variables did not follow a normal distribution, quantitative and ordinal variables were compared between the control and exposed groups using the Mann-Whitney test.

Binary variables (e.g., present/absent, yes/no, and regular/irregular) were compared between groups using Fisher's exact test based on contingency tables. Quantitative variables measured at multiple thoracic sites were compared across sites using the Kruskal–Wallis test. When no statistically

significant differences among sites were detected, measurements were pooled and overall median values were calculated for subsequent analyses.

The correlations between hair nicotine concentration and qualitative and quantitative variables that differed significantly between the exposed and control groups were assessed using Spearman's correlation coefficient. Descriptive statistics included the median, interquartile range (IQR), and skewness of the variables evaluated. Statistical significance was set at $P < 0.05$ for all analyses.

Declarations

Data availability. All data supporting the findings of this study are available within the paper and any additional required data may be requested from the manuscript's authors.

Acknowledgements. The authors would like to thank for São Paulo Research Foundation (FAPESP/CAPES) (grand process numbers: 2022/07366-0 and 2023/05110-0) and National Council for Scientific and Technological (CNPq) for funding the research (productivity scholarship: 305182/2020-0), and owners and breeders of the dogs participating in this study. The authors also thank Prof. Thiago Henrique Annibale Vendramini and the Research Center for Dog and Cat Nutrology for their assistance.

Author contributions. G.S.R.F., R.A.R.U, M.A.R.F., and C.E.A.: conception and design; G.S.M.F., A.P.S., L.P.N.A., C.G.B.S., G.C.L.E., A.L.B., J.J.P.N., F.G.T, C.A.F.O., R.A.R.U., M.A.R.F., C.E.A.: acquisition of Data; G.S.M.F., G.C.L.E., F.G.T., C.A.F.O., R.A.R.U. and M.A.F.R.: analysis and interpretation of data; G.S.M.F., A.C.M.E., R.A.R.U., M.A.F.R. and C.E.A.: drafting the article; all authors approved the final version of the completed article. All authors approved the final version of the completed article.

Competing Interests. The authors declare no competing interests.

Correspondence and requests for materials should be addressed to G.S.M.F.

References

1. World Health Organization. Tobacco. *World Health Organization.* (2025). https://www.who.int/news-room/fact-sheets/detail/tobacco
2. Al-Sayed, E. M. & Ibrahim, K. Second-hand tobacco smoke and children. *Toxicol. Ind. Health*. **30**, 635–644. 10.1177/0748233712462473 (2014).
3. Ka, D. et al. Association between passive smoking and atopic dermatitis in dogs. *Food Chem. Toxicol.* **66**, 329–333. 10.1016/j.fct.2014.01.015 (2014).
4. Food and Drug Administration. Be Smoke-free and Help Your Pets Live Longer, Healthier Lives. *Food and Drug Administration.* (2022). https://www.fda.gov/animal-veterinary/animal-health-literacy/be-smoke-free-and-help-your-pets-live-longer-healthier-lives

5. Yamaya, Y., Sugiya, H. & Watari, T. Tobacco exposure increased airway limitation in dogs with chronic cough. *Vet. Rec*. **174**, 18–18. 10.1136/vr.101810 (2014).
6. Reif, J. S., Dunn, K., Ogilvie, G. K. & Harris, C. K. Passive smoking and canine lung cancer risk. *Am. J. Epidemiol.* **135**, 234–239. 10.1093/oxfordjournals.aje.a116276 (1992).
7. Reif, J. S., Bruns, C. & Lower, K. S. Cancer of the nasal cavity and paranasal sinuses and exposure to environmental tobacco smoke in pet dogs. *Am. J. Epidemiol.* **147**, 488–492. 10.1093/oxfordjournals.aje.a009475 (1998).
8. Moraes, S. I. R. et al. Elastographic and ultrasound findings of the dog's kidneys exposed to cigarette smoke. *Braz J. Vet. Med.* **47**, e003525. 10.29374/2527 - 2179.bjvm003525 (2025).
9. Gomes, F. G. E. et al. Ultrasonographic and elastographic findings of the liver of dogs exposed to cigarette smoke. *Braz J. Vet. Med.* **48**, e005026–e005026. 10.29374/2527 - 2179.bjvm00502 (2026).
10. Vassallo, R. & Ryu, J. H. Tobacco smoke–related diffuse lung diseases. *Sem Respir Crit. Care Med.* **29**, 643–650. 10.1055/s-0028-1101274 (2008).
11. Reinero, C. Interstitial lung diseases in dogs and cats part I: The idiopathic interstitial pneumonias. *Vet. J.* **243**, 48–54. 10.1016/j.tvjl.2018.11.010 (2019).
12. Donovan, T. A. & Daverio, H. Histologic patterns of chronic interstitial lung diseases in dogs, cats, and humans: a review. *J. Vet. Diagn. Invest.* **38**, 724–744. 10.1177/10406387261421554 (2026).
13. Spasov, K., Kunovska, M. & Dimov, D. Lung patterns in the dog - normal and pathological. *Trad Mod. Vet. Med.* **3**, 7–14 (2018).
14. Łobaczewski, A. et al. Lung ultrasound for imaging of B-Lines in dogs and cats — A prospective study investigating agreement between three types of transducers and the accuracy in diagnosing cardiogenic pulmonary edema, pneumonia and lung neoplasia. *Animals* **11**, 3279–3294. 10.3390/ani11113279 (2021).
15. Zhou, B., Bartholmai, B. J., Kalra, S., Osborn, T. G. & Zhang, X. Lung US surface wave elastography in interstitial lung disease staging. *Radiology* **291**, 479–484. 10.1148/radiol.2019181729 (2019).
16. Huang, S. et al. Evaluation of connective tissue disease-related interstitial lung disease using ultrasound elastography: a preliminary study. *Quant. Imaging Med. Surg.* **12**, 3778–3791. 10.21037/qims-21-1205 (2022).
17. Dietrich, D. F. et al. Effects of passive smoking on heart rate variability, heart rate and blood pressure: an observational study. *Int. J. Epidemiol.* **36**, 834–840. 10.1093/ije/dym031 (2007).
18. Makris, T. K. et al. Association of passive smoking with masked hypertension in clinically normotensive nonsmokers. *Am. J. Hypertens.* **22**, 853–859 (2009).
19. Münzel, T., Area, F., Rajagopalan, S. & Lüscher, T. Nicotine and the cardiovascular system: unmasking a global public health threat. *Eur. Heart J.* **47**, 1764–1781. 10.1093/eurheartj/ehaf1010 (2025).
20. Erturk, N. & Karababa, H. N. Comparative effects of electronic and traditional cigarette use on pulmonary function, autonomic regulation, and exercise capacity in young adults. *Ir. J. Med. Sci.* **195**, 695–702. 10.1007/s11845-025-04271-1 (2026).

21. Zeng, S., Dunn, M., Gold, W. M., Kizer, J. R. & Arjomandi, M. Remote exposure to secondhand tobacco smoke is associated with lower exercise capacity through effects on oxygen pulse, a proxy of cardiac stroke volume. *BMJ Open. Respirator Res.* **9**, e001217. 10.1136/bmjresp-2022-001217 (2022).
22. Aviles-Solis, J. C. et al. Prevalence and clinical associations of wheezes and crackles in the general population: the Tromsø study. *BMC Pum Med.* **19**, 173–183. 10.1186/s12890-019-0928-1 (2019).
23. Kogan, D. A., Johnson, L. R., Jandrey, K. E. & Polland, R. E. Clinical, clinicopathologic, and radiographic findings in dogs with aspiration pneumonia: 88 cases (2004–2006). *J. Am. Vet. Med. Assoc.* **233**, 1742–1747. 10.2460/javma.233.11.1742 (2008).
24. Detorakis, E. E., Lasithiotaki, I., Dailiani, K. & Raissaki, M. HRCT findings in secondhand smokers with respiratory symptoms. *Jpn J. Radiol.* **41**, 153–163. 10.1007/s11604-022-01336-4 (2023).
25. Mohammad, R. H. & Al Kattan, M. A. Smoking perturbed liver machinery relevant to mitochondrial functions. *Mil Med. Sci. Lett.* **92**, 333–338. 10.31482/mmsl.2022.052 (2023).
26. Cerón, J. J., Eckersall, P. D. & Martínez-Subiela, S. Acute phase proteins in dogs and cats: current knowledge and future perspectives. *Vet. Clin. Pathol.* **34**, 85–99. 10.1111/j.1939-165x.2005.tb00019.x (2005).
27. Mantovani, A. & Garlanda, C. Humoral innate immunity and acute-phase proteins. *N Engl. J. Med.* **388**, 439–452. 10.1056/NEJMra2206346 (2023).
28. Venn, A. & Britton, J. Exposure to secondhand smoke and biomarkers of cardiovascular disease risk in never-smoking adults. *Circulation* **115**, 990–995. 10.1161/CIRCULATIONAHA.106.648469 (2007).
29. Jefferis, B. J. et al. Secondhand smoke (SHS) exposure is associated with circulating markers of inflammation and endothelial function in adult men and women. *Atherosclerosis* **208**, 550–556. 10.1016/j.atherosclerosis.2009.07.044 (2010).
30. Chattopadhyay, D. et al. Inflammasome-primed neutrophils aggravate atherosclerosis in cigarette smoking. *Circ. Res.* **139**, e327714. 10.1161/CIRCRESAHA.125.327714 (2026).
31. Ahmed, I. A., Mohammed, M. A., Hassan, H. M. & Ali, I. A. Relationship between tobacco smoking and hematological indices among Sudanese smokers. *J. Health Popul. Nutr.* **43**, 5. 10.1186/s41043-023-00493-0 (2024).
32. Khudhur, Z. O. et al. The effects of heavy smoking on oxidative stress, inflammatory biomarkers, vascular dysfunction, and hematological indices. *Sci. Rep.* **15**, 18251. 10.1038/s41598-025-03075-8 (2025).
33. Çekici, Y., Yılmaz, M. & Seçen, Ö. New inflammatory indicators: association of high eosinophil-to-lymphocyte ratio and low lymphocyte-to-monocyte ratio with smoking. *J. Int. Med. Res.* **47**, 4292–4303. 10.1177/0300060519862077 (2019).
34. Ghadirzadeh, E. et al. The association between smoking profile, leukocyte count, and inflammatory indices in males: a cross-sectional analysis of the TABARI cohort study at enrollment phase. *Inhal Toxicol.* **37**, 146–155. 10.1080/08958378.2025.2499825 (2025).

35. Sangani, R. G., Deepak, V., Anwar, J., Patel, Z. & Ghio, A. J. Cigarette smoking, and blood monocyte count correlate with chronic lung injuries and mortality. *Int. J. Chron. Obstruct Pulmon Dis.* **18**, 431–446. 10.2147/COPD.S397667 (2023).
36. Dennis, R. Radiological assessment of lung disease in small animals: 1. Bronchial and vascular patterns. *Pract.* **30**, 182–189. 10.1136/inpract.30.4.182 (2008).
37. Thrall, D. E. Canine and feline pleural space in Textbook of Veterinary Diagnostic Radiology (ed Thrall, D. E.) 670–683 (Elsevier, (2018).
38. Burnotte, P., Graziano, N. & Gommeren, K. A retrospective study on parapneumonic effusion in 130 dogs with a clinical diagnosis of pneumonia. *Front. Vet. Sci.* **10**, 1144148. 10.3389/fvets.2023.1144148 (2023).
39. Dennis, R., Kirberger, R. M., Barr, F. & Wrigley, R. H. Other thoracic structures - pleural cavity, mediastinum, thoracic oesophagus, thoracic wall in Handbook of Small Animal Radiology and Ultrasound: Techniques and Differential Diagnoses 2nd (eds Dennis, R., Kirberger, R. M., Barr, F. & Wrigley, R. H.) 199–228 (Saunders Elsevier, (2010).
40. Jaeger, G. et al. Haemorrhagic pneumonia in sled dogs caused by *Streptococcus equi* subsp. *zooepidemicus*—one fatality and two full recoveries: a case report. *Acta Vet. Scand.* **55**, 67. 10.1186/1751-0147-55-67 (2013).
41. Delle Sedie, A. et al. Interstitial lung disease: does it represent a real comorbidity in spondyloarthritis patients? Results from an ultrasound monocentric pilot study. *J. Clin. Med.* **14**, 5632. 10.3390/jcm14165632 (2025).
42. Mansour, O. F., Agha, M. A., Al-Asdody, A., Mehana, N. S. & Habib, R. M. Sonographic features of idiopathic pulmonary fibrosis. *Egypt. J. Chest Dis. Tuberc*. **67**, 50–55. 10.4103/ejcdt.ejcdt_38_17 (2018).
43. Soliveres, E. et al. A high number of ring-down artefacts and an irregular pleural surface are more commonly observed in WHWTs suffering from idiopathic pulmonary fibrosis compared to control WHWTs. *Animals* **15**, 2964. 10.3390/ani15202964 (2025).
44. Oricco, S., Medico, D., Tommasi, I., Bini, R. M. & Rabozzi, R. Lung ultrasound score in dogs and cats: a reliability study. *J. Vet. Intern. Med.* **38**, 336–345. 10.1111/jvim.16956 (2024).
45. Makena, P., Kikalova, T., Prasad, G. L. & Baxter, S. A. Oxidative stress and lung fibrosis: towards an adverse outcome pathway. *Int. J. Mol. Sci.* **24**, 12490. 10.3390/ijms241512490 (2023).
46. Raiteri, A. et al. Lung ultrasound is often, but not always, normal in healthy subjects: considerations for COVID-19 pandemic. *Diagnostics* **11**, 82. 10.3390/diagnostics11010082 (2021).
47. Song, H. & Lee, J. Differences of low-dose chest computed tomography findings between smokers and nonsmokers based on smoking cessation program. *Iran. J. Radiol.* **15**, e64340. 10.5812/iranjradiol.64340 (2018).
48. Li, S. J. et al. Presence of pleural adhesions can predict conversion to thoracotomy and postoperative surgical complications in patients undergoing video-assisted thoracoscopic lung cancer lobectomy. *J. Thorac. Dis.* 10, 416–431 0.21037/jtd.2017.12.70 (2018).

49. Cassanelli, N. et al. Accuracy of transthoracic ultrasound for the detection of pleural adhesions. *Eur. J. Cardiothorac. Surg.* **42**, 813–818. 10.1093/ejcts/ezs144 (2012).

50. Fukuda, K. et al. Prevalence and characteristics of minimal pleural fluid on screening chest MRI. *Respir Investig*. **62**, 1109–1116. 10.1016/j.resinv.2024.09.014 (2024).

51. Rigot, M., Boysen, S. R., Maseru, I. & Letendre, J. A. Evaluation of B-lines with 2 point-of-care lung ultrasound protocols in cats with radiographically normal lungs. *J. Vet. Emerg. Crit. Care*. **34**, 143–152. 10.1111/vec.13360 (2024).

52. Zoneff, E. R. et al. The prevalence of lung surface abnormalities in a healthy population as detected by a screening lung ultrasound protocol: comparison between young and older volunteers. *Australas J. Ultrasound Med.* **22**, 129–137. 10.1002/ajum.12124 (2019).

53. Zierenberg-Ripoll, A. et al. Association between environmental factors including second-hand smoke and primary lung cancer in dogs. *J. Small Anim. Pract.* **59**, 343–350. 10.1111/jsap.12778 (2018).

54. Freedman, N. D., Leitzmann, M. F., Hollenbeck, A. R., Schatzkin, A. & Abnet, C. C. Cigarette smoking and the subsequent risk of lung carcinoma in the men and women of a large prospective cohort study. *Lancet Oncol.* **9**, 649–656. 10.1016/S1470-2045(08)70154-2 (2008).

55. Possenti, I. et al. Association between second-hand smoke exposure and lung cancer risk in never-smokers: a systematic review and meta-analysis. *Eur. Respir Rev.* **33**, 240077. 10.1183/16000617.0077-2024 (2024).

56. Abdullayeva, Z. et al. The role of lung ultrasound and ultrasound elastography in diagnosis of interstitial lung diseases. *Tuberk Toraks*. **72**, 202402873. 10.5578/tt.202402873 (2024).

57. Jones, M. G. et al. Nanoscale dysregulation of collagen structure-function disrupts mechano-homeostasis and mediates pulmonary fibrosis. *eLife* **7**, e36354. 10.7554/eLife.36354 (2018).

58. Knottenbelt, C. M., Bawazeer, S., Hammond, J., Mellor, D. & Watson, D. G. Nicotine hair concentrations in dogs exposed to environmental tobacco smoke: a pilot study. *J. Small Anim. Pract.* **53**, 623–626. 10.1111/j.1748-5827.2012.01284.x (2012).

59. Dai, T. & Silverstein, T. P. Analysis of nicotine in dog hair: significant dose-response to passive smoke. *J. Undergrad. Chem. Res.* **21**, 7–10 (2022).

60. Balmes, J. R. et al. Annual average ambient particulate matter exposure estimates, measured home particulate matter, and hair nicotine are associated with respiratory outcomes in adults with asthma. *Environ. Res.* **129**, 1–10. 10.1016/j.envres.2013.12.007 (2014).

61. Wang, Y. et al. Respiratory symptoms and urinary cotinine levels in pre-school children exposed to environmental tobacco smoke. *Front. Public. Health*. **8**, 587193. 10.3389/fpubh.2020.587193 (2021).

62. Groppetti, D., Pizzi, G., Pecile, A., Bronzo, V. & Mazzola, S. M. Cotinine as a sentinel of canine exposure to tobacco smoke. *Animals* **13**, 693. 10.3390/ani13040693 (2023).

63. Chan, S. S. C. et al. Secondhand smoke exposure and maternal action to protect children from secondhand smoke: pre- and post-smokefree legislation in Hong Kong. *PLoS ONE*. **9**, e105781. 10.1371/journal.pone.0105781 (2014).

64. Wipfli, H. et al. Secondhand smoke exposure among women and children: evidence from 31 countries. *Am. J. Public. Health*. **98**, 672–679. 10.2105/AJPH.2007.126631 (2008).
65. Heatherton, T. F., Kozlowski, L. T., Frecker, R. C. & Fagerström, K. O. The Fagerström Test for Nicotine Dependence: a revision of the Fagerström Tolerance Questionnaire. *Br. J. Addict.* **86**, 1119–1127. 10.1111/j.1360-0443.1991.tb01879.x (1991).
66. Papadopoulou, E. et al. The Fagerström Test for Nicotine Dependence, as a prognostic factor, in current smokers with and without COPD: a cross-sectional study in northern Greece. *Chronic Respir Dis.* **21** 10.1177/14799731241235213 (2024).
67. Gutenkunst, S. L. & Bell, M. L. Managing missing items in the Fagerström Test for Nicotine Dependence: a simulation study. *BMC Med. Res. Methodol.* **22** 10.1186/s12874-022-01637-2 (2022).
68. Pavelski, M., Feliciano, M. A. R. & Sistema respiratório in *Diagnóstico por Imagem em Cães e Gatos* (ed. Feliciano, M. A. R.) 1130–1177 (MedVet, 2025).
69. Boysen, S. R. & Lisciandro, G. R. The use of ultrasound for dogs and cats in the emergency room: AFAST and TFAST. *Vet. Clin. North. Am. Small Anim. Pract.* **43**, 773–797 (2013).
70. Lisciandro, G. R., Fosgate, G. T. & Fulton, R. M. Frequency and number of ultrasound lung rockets (B-lines) using a regionally based lung ultrasound examination named Vet BLUE (veterinary bedside lung ultrasound exam) in dogs with radiographically normal lung findings. *Vet. Radiol. Ultrasound*. **55**, 315–322 (2014).
71. Assis, A. R. & Feliciano, M. A. R. Ultrassonografia torácica extracardíaca in *Ultrassonografia em Cães e Gatos* (eds Feliciano, M. A. R., Assis, A. R. & Vicente, W. R. R.) 426–474 (MedVet, 2019).
72. Maronezi, M. C., Feliciano, M. A. R. & Vicente, W. R. R. Elastografia e ultrassonografia contrastada in *Ultrassonografia em Cães e Gatos* (eds Feliciano, M. A. R., Assis, A. R. & Vicente, W. R. R.) 33–42 (MedVet, 2019).
73. Bawazeer, S., Watson, D. G. & Knottenbelt, C. Determination of nicotine exposure in dogs subjected to passive smoking using methanol extraction of hair followed by hydrophilic interaction chromatography in combination with Fourier transform mass spectrometry. *Talanta* **88**, 408–411. 10.1016/j.talanta.2011.11.008 (2012).

Figures

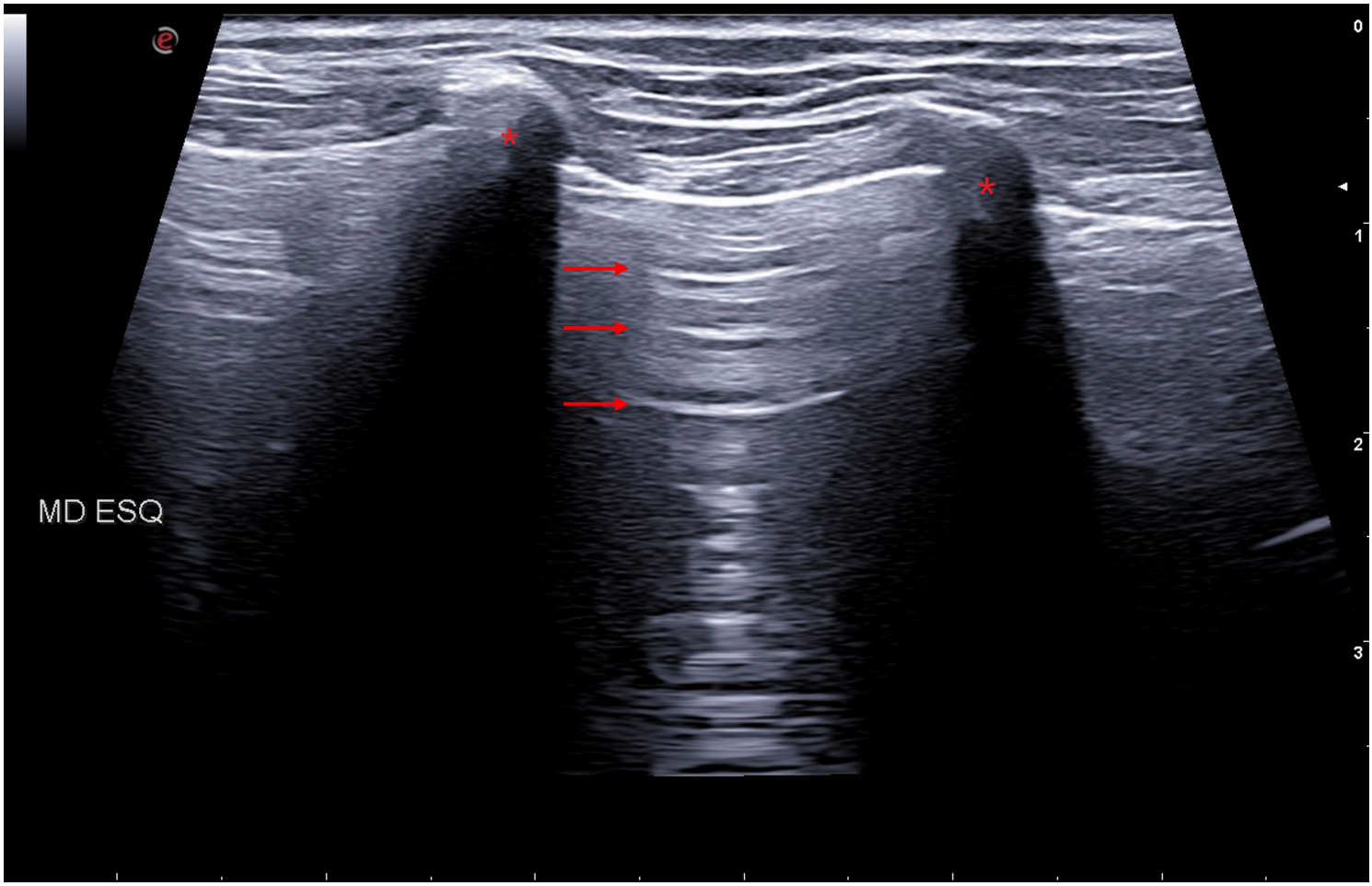


Figure 1

B-mode ultrasonographic image of the pulmonary region showing the pleuropulmonary interface (green arrow), A-lines (red arrows), and the acoustic shadows of the ribs (red asterisks).

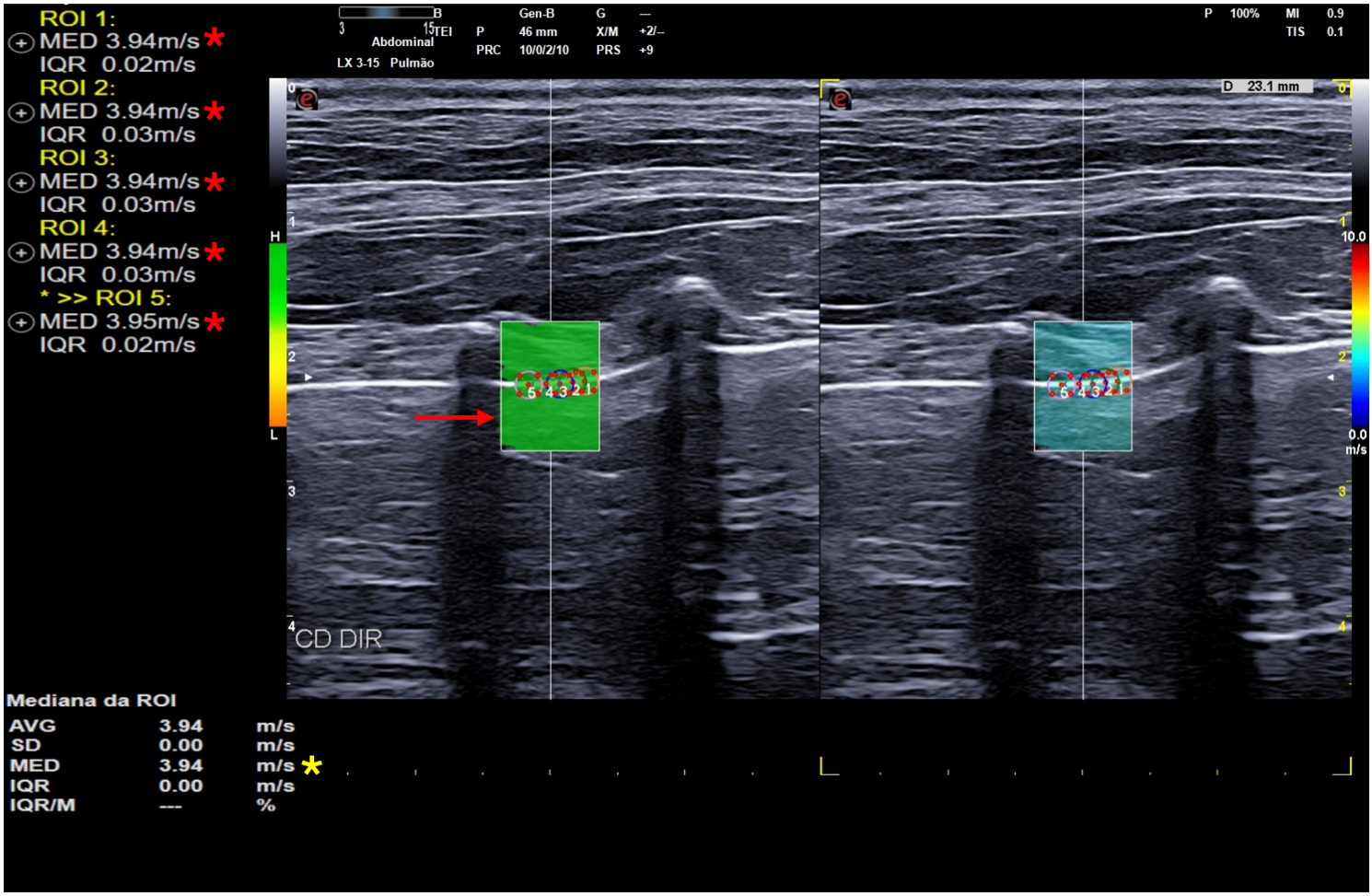


Figure 2

Qualitative and quantitative elastography images of the pleuropulmonary interface, showing the reliability map (in green; thin red arrow) and its color scale (thick red arrow), the elastogram (thin yellow arrow) and its color scale (thick yellow arrow), the regions of interest (ROIs; red circles numbered 1 to 5), and the respective median (MED) values of shear-wave propagation velocity (m/s) (red asterisks), as well as the median of the five ROIs (yellow asterisk) from a dog belonging to the control exposited.

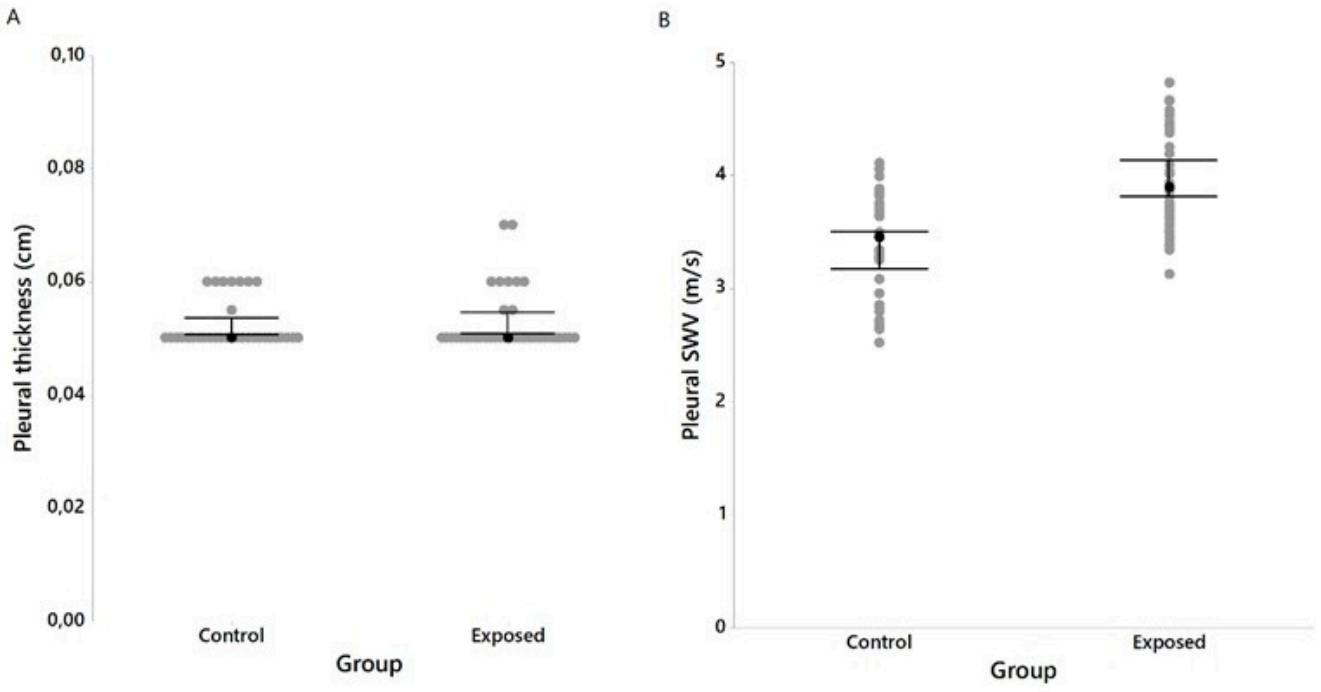


Figure 3

Scatter plot of the global pleural thickness (A) and the global shear-wave propagation velocity (SWV) of the pleuropulmonary interface (PPI) (B) in dogs from the control and exposed groups.

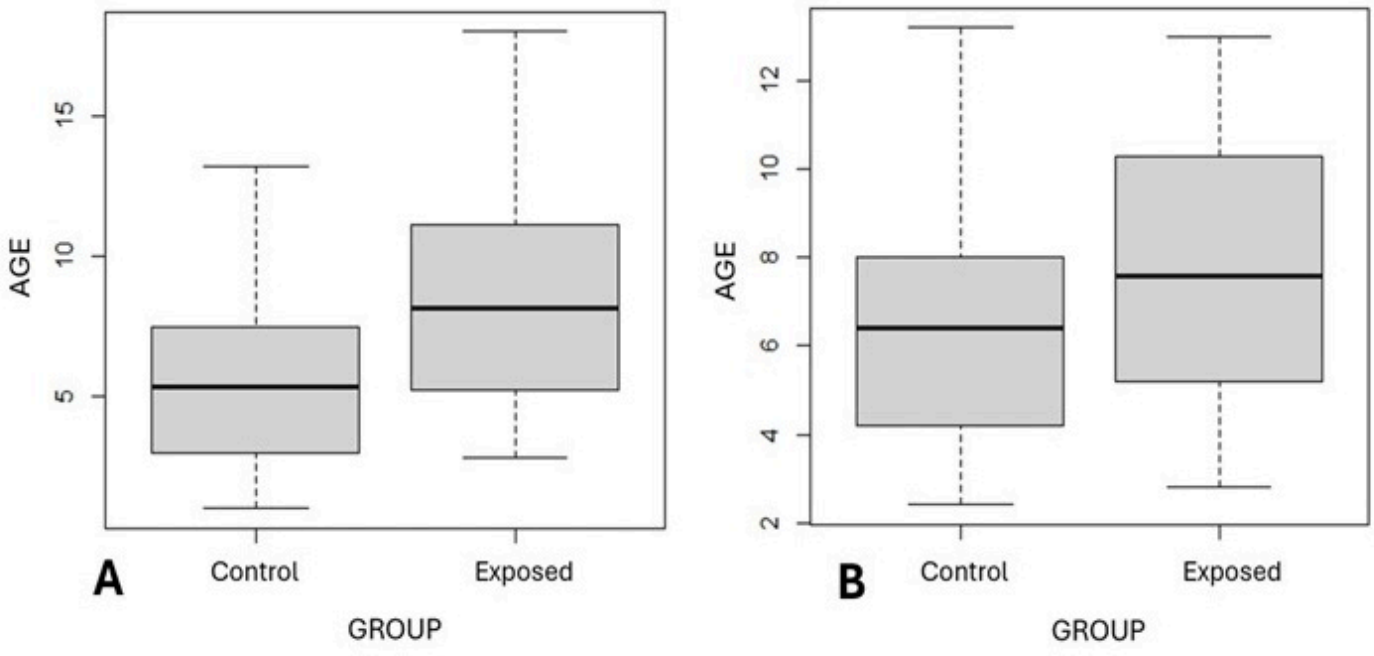


Figure 4

Boxplot of the age distribution of dogs in the control and exposed groups before (A) and after (B) the exclusion of animals with discrepant ages.

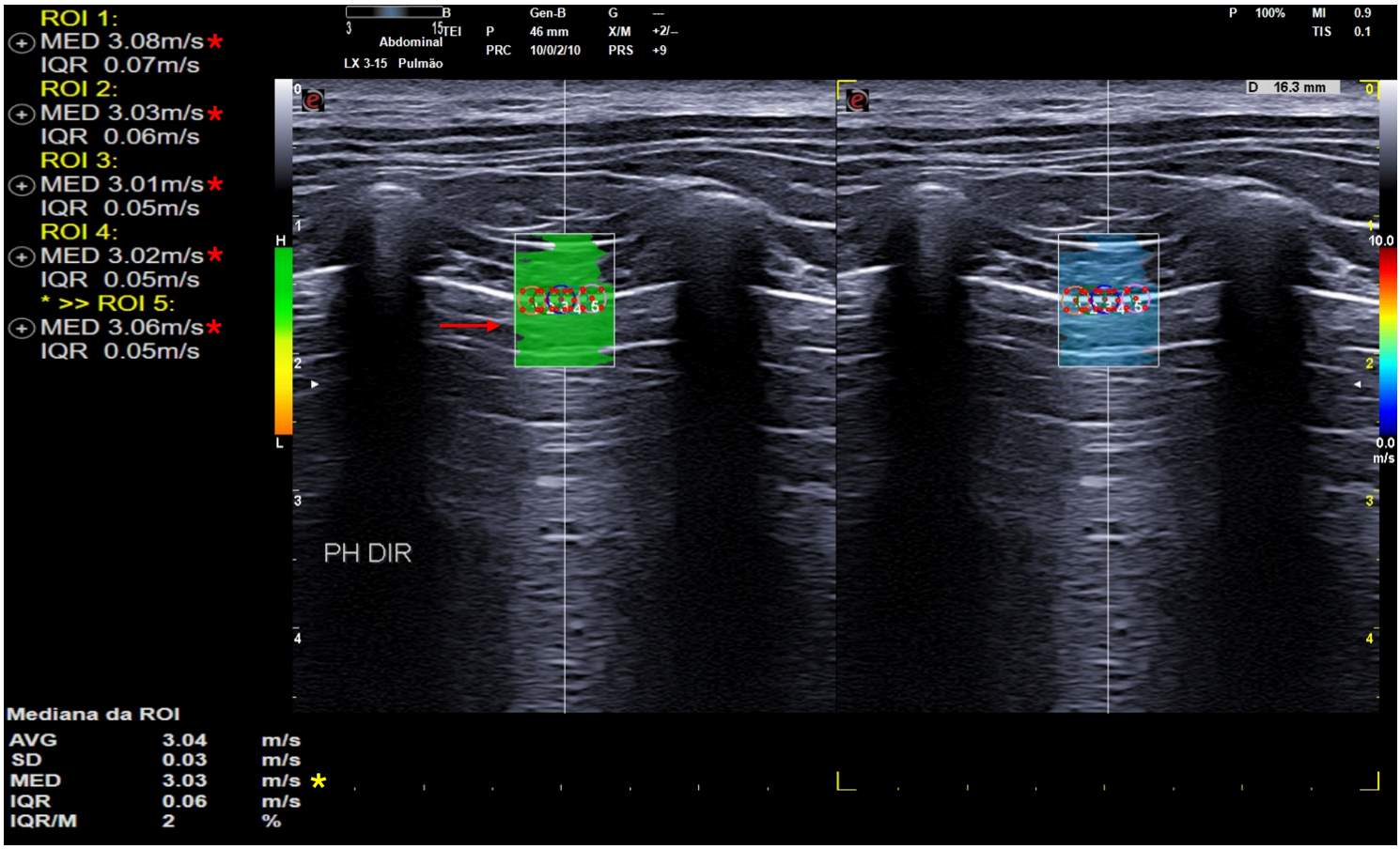


Figure 5

Elastography image of the pleuropulmonary interface in the right perihilar pulmonary region (PH R), showing the reliability map (in green; red arrow), the regions of interest (ROIs; red circles numbered 1 to 5), and the respective median (MED) values of shear-wave propagation velocity (m/s) (red asterisks), as well as the median of the five ROIs (yellow asterisk), from a dog belonging to the control group.